

## SOFC Anode Fabricated by Magnetically Aligning of Ni Particles

K. Nagato<sup>a</sup>, N. Shikazono<sup>b</sup>, A. Weber<sup>c</sup>, D. Klotz<sup>c</sup>, M. Nakao<sup>a</sup>, and E. Ivers-Tiffée<sup>c</sup>

<sup>a</sup> Department of Mechanical Engineering, The University of Tokyo, Tokyo 113-8656, Japan

<sup>b</sup> Institute of Industrial Science (IIS), The University of Tokyo, Tokyo 153-8505, Japan

<sup>c</sup> Institut für Werkstoffe der Elektrotechnik (IWE), Karlsruher Institut für Technologie (KIT), 76131 Karlsruhe, Germany

Ni particles are aligned by magnetic field during the drying process after screen-printing Ni/8YSZ (yttria-stabilized zirconia) paste. By applying a magnetic field, Ni particles are magnetically polarized, attracted to each other, and align along the magnetic field. It is proposed, that not only tortuosity of Ni but also that of YSZ and of pores is decreased. Symmetrical half cells are fabricated with 15- $\mu\text{m}$ -thick anodes and 200- $\mu\text{m}$ -thick YSZ electrolytes. A current collector made of porous Ni with a thickness of approximately 5  $\mu\text{m}$  was printed on top of each anode. The microstructural changes in the anodes are analyzed by scanning electron microscopy. Impedance measurements are performed at 700°C in H<sub>2</sub>/H<sub>2</sub>O atmospheres containing 10% and 60% H<sub>2</sub>O. The initial polarization resistance was decreased after applying a magnetic field of 100 mT by up to 25%. However, with higher magnetic field, the polarization resistance increases, which might be explained by a pronounced increase of the surface roughness with 30  $\mu\text{m}$  peak-to-valley, causing current constriction.

### Introduction

A solid oxide fuel cell (SOFC) is one of the most promising energy conversion devices because of its high efficiency (1). The state-of-the-art anode consists of three phases: yttria-stabilized zirconia (YSZ), Ni and pores. The electrooxidation reaction occurs at the three-phase boundary (TPB). Usually, YSZ and Ni and pores are randomly distributed, and their individual tortuosity factor is  $>1$  (2, 3). The tortuosity factor of 1 means the ideal structure, in which the path has a constant cross-sectional shape and stretches in the thickness direction. State-of-the-art anodes show tortuosity factors for Ni and YSZ of larger than 5, which were qualified by focused ion beam-scanning electron microscopy (FIB-SEM) (2, 3). With a lower tortuosity factor, it is proposed that the resistances of electrons, oxide ions and gases can be lowered. In this study, to obtain paths with lower tortuosity factors, we present a method of aligning Ni particles by a magnetic field. When a magnetic field is applied to the anode, Ni particles are magnetically polarized and attracted to each other, resulting in an alignment in the thickness direction.

Impedance measurements are performed with symmetrical half cells which are made by screen-printing paste containing YSZ and Ni particles and subsequent drying process with different magnetic fields. The resulting anode microstructures are observed by SEM.

## Experimental

The anode was prepared by screen-printing. Ni powder from Kojundo Kagaku (NIE01PB) and 8 mol% YSZ from Tosoh (TZ-8Y) were used as starting materials. The average particle sizes were 1  $\mu\text{m}$  for both materials. After the electrodes were applied on the 200- $\mu\text{m}$ -thick 8YSZ electrolyte from Itochu, magnetic fields, 0, 100, 200, 290 mT, were applied in the direction of thickness in an atmospheric oven with 90°C. During this process, the viscosity of the paste becomes lower than in room temperature and Ni particles can move more easily, and the solvent is evaporated at the same time. We confirmed that the solvent was completely evaporated in 30 min in 90°C oven. After the solvent was evaporated, the electrode was pasted on the other side of the electrolyte as well. The resulting average thickness of the electrodes was approximately 15  $\mu\text{m}$  for each side. And then, we additionally pasted Ni slurry as current collectors on both anodes. The thickness of this current-collecting layer was approximately 5  $\mu\text{m}$ . The solvent of Ni was also evaporated in the oven. After sintering (1300°C, 5 h) and reduction in the testing furnace, the anode consists of 50 vol% Ni and 50 vol% YSZ of total solid.

For electrochemical testing the symmetric half cells the same setup was used as in (4, 5). Two Ni-meshes (>99.2% Ni, 2500 meshes/cm<sup>2</sup>, 0.065 mm wires) were used as current collectors. A weight of 120 g ensured a reliable contacting. The sintered samples were reduced in this furnace at 800°C for 2 h immediately before the measurement. The concentration of the fuel gas H<sub>2</sub> and H<sub>2</sub>O were verified 90:10 and 40:60. The impedance measurements with this verification of gas components were carried out for three times in 700°C. We compared the experimental impedance spectra of the third one.

## Results and Discussion

### SEM Observation of the Anodes

Fig. 1 shows cross-sectional SEM images of anodes with three different magnetic fields, 0(a), 100(b), 200(c), and 290 mT(d). These samples were used for the measurement. We confirm that the SEM images of the samples before measurement and that after measurement were similar. In Fig. 1(b), the Ni path has some anisotropy in the thickness direction. In Figs. 1(c, d), the surface of anode has periodic convex-and-concaves with 150  $\mu\text{m}$  pitch and 30  $\mu\text{m}$  peak-to-valley although their Ni paths have more anisotropy. In some areas the electrolyte is exposed to the ambient. The pattern of the surface roughness corresponds to those of mesh of screen-printing mask. Therefore, it is considered that the polarized Ni particles are attracted strongly in each island which was originally formed by screen printing, and not only Ni particles but also YSZ and liquid at lower areas are pulled together to the higher area. However, in each island, special paths of Ni, i.e. Ni chains, stretched in the thickness direction, are observed in the magnified images.

The thickness and average particle size in Ni current-collecting layers are around 5  $\mu\text{m}$ . Although the original particle size of Ni was 1  $\mu\text{m}$  in average, which is the same as that in the anode, it became larger during reduction process at 800 °C. However, they have a good connection to the Ni paths in the anode and proper porosity for gas diffusion.

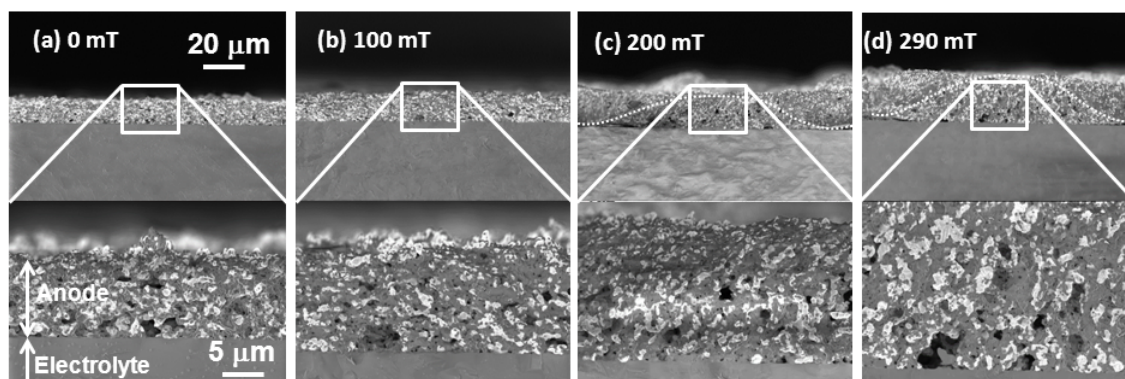


Figure 1. SEM images of cross sections of anode with no magnetic field (a), 100 mT (b), 200 mT (c), and 290 mT (d). Dotted lines in (c) and (d) indicate upper surfaces of the anode cross sections.

### Impedance Measurements

Impedance measurements with these symmetrical cells are carried out at 700 °C and 10% and 60% water vapor contents. Fig. 2 shows impedance spectra and corresponding distribution of relaxation times (DRTs) (6). The polarization resistances corresponding to single anodes, which are calculated from the impedance spectra, are plotted in Fig. 3. In the results with 10/60% H<sub>2</sub>O, the total polarization resistance decreases from 2.2/0.79 to 1.7/0.63 Ωcm<sup>2</sup> with 100 mT magnetic field, however, it increases to 2.1/0.88 and 2.4/1.0 Ωcm<sup>2</sup> with further increasing the magnetic fields to 200 and 290 mT, respectively. We propose that the improvement measured at samples exposed to 100 mT is caused by a reorganization of the TPBs, mainly introduced by the alignment of Ni particles.

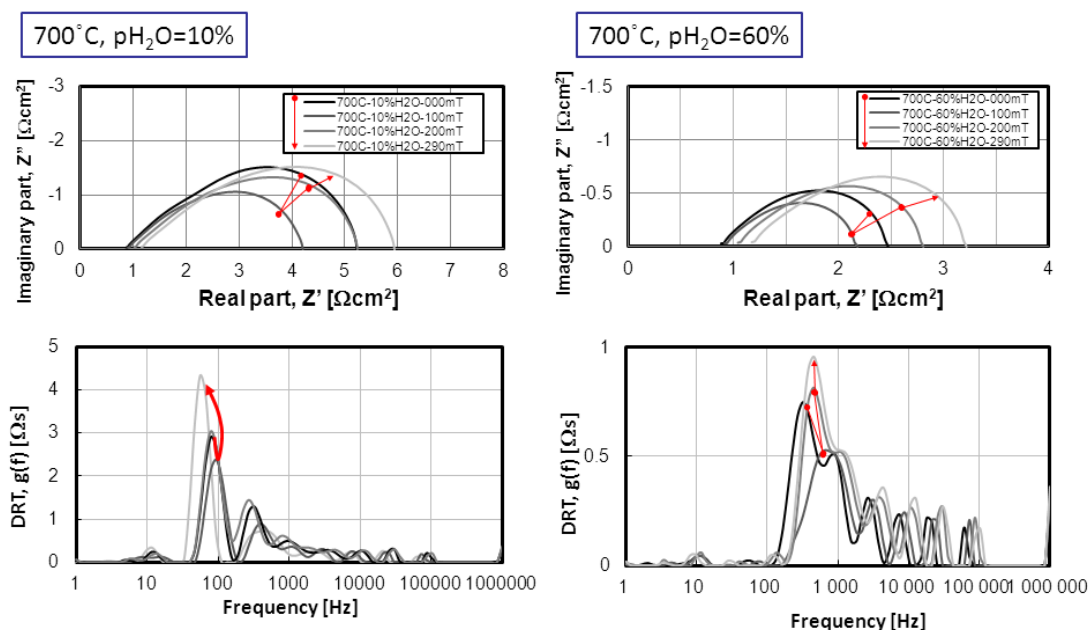


Figure 2. Impedance spectra and corresponding DRTs of symmetrical cells with different magnitude of magnetic field applied, at 700 °C,  $p_{\text{H}_2\text{O}} = 10\%$  and  $60\%$ .

However, with a magnetic field of 290 mT, the polarization resistance increases, which might be explained by a pronounced increase of the surface roughness with 20  $\mu\text{m}$  peak-to-valley, causing current constriction effects. In the DRTs in Fig. 2, the main peak frequencies of samples with no magnetic field and 100 mT shift from 80/320 to 90/780 Hz with 10/60% $\text{H}_2\text{O}$  and the main peak areas decrease, respectively.

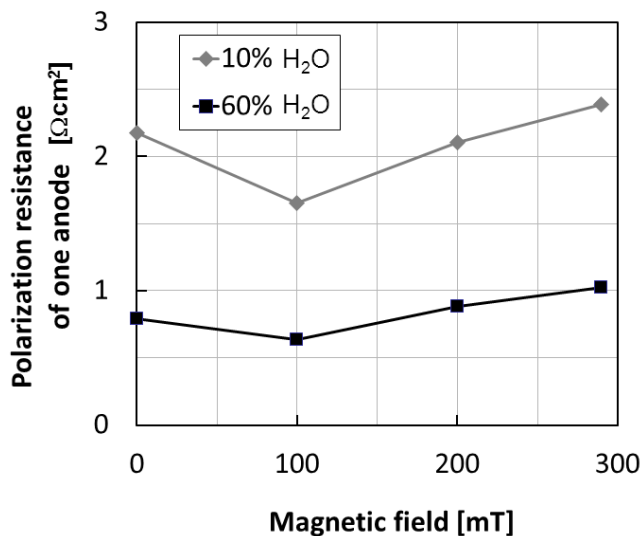


Figure 3. Polarization resistance corresponding one anode as a function of magnetic field at  $\text{pH}_{2\text{O}} = 10\%$  and  $60\%$ .

### Conclusions

We proposed the aligning method of Ni particles in a screen-printed Ni/YSZ anode using magnetic field (0, 100, 200, 290 mT). Impedance measurement at  $700^\circ\text{C}$  and 10% and 60%  $\text{H}_2\text{O}$  with symmetrical cells revealed a positive effect of the magnetic field on the measured total polarization resistance with a 25% lower polarization resistance at 100 mT than without magnetic field. However, further increases of the magnetic field to 200 and 290 mT lead to approximately 30% and 45% higher resistances, respectively. 3D-microstructure reconstruction by focused ion beam tomography is necessary to shed light on the correlation between tortuosity, respectively three-phase boundary characteristics, and measured changes in total polarization resistance.

### Acknowledgments

We would like to thank Ms. Sarah van der Hazel and Mrs. Sylvia Schöllhammer (IWE, KIT) for their assistance in preparation of slurry and screen-printing, and Dr. Jan Hayd (IWE, KIT) for his helpful discussion. This study was partly supported by JSPS KAKENHI Grant Numbers 24686019, 24246027 and Global Center-of-Excellence for Mechanical System Innovation (GCOE-MSI) from the Ministry of Education, Culture, Sports, Science and Technology (MEXT), Japan.

## References

1. S. C. Singhal and K. Kendall, *High-temperature solid oxide fuel cells: Fundamentals, design and applications* (Elsevier Science, Oxford, 2003).
2. H. Iwai, N. Shikazono, T. Matsui, H. Teshima, M. Kishimoto, R. Kishida, D. Hayashi, K. Matsuzaki, D. Kanno, M. Saito, H. Muroyama, K. Eguchi, N. Kasagi, and H. Yoshida, *J. Power Sources*, **195**, 955 (2010).
3. N. Shikazono, D. Kanno, K. Matsuzaki, H. Teshima, S. Sumio, and N. Kasagi, *J. Electrochem. Soc.*, **157**, B665 (2010).
4. S. Gewies, W. G. Bessler, V. Sonn, and E. Ivers-Tiffée, *ECS Trans.*, **7**(1) 1573 (2007).
5. V. Sonn, A. Leonide, and E. Ivers-Tiffée, *J. Electrochem. Soc.*, **155**, B675 (2008).
6. H. Schichlein, A. C. Müller, M. Voigts, A. Krügel, and E. Ivers-Tiffée, *J. Appl. Electrochem.*, **32**, 875 (2002).